OPEN

Deep learning quantification reveals a fundamental prognostic role for ductular reaction in biliary atresia

Iiris Nyholm[1,2] | Nelli Sjöblom[3] | Marjut Pihlajoki[2] | Maria Hukkinen[1] |
Jouko Lohi[3] | Päivi Heikkilä[3] | Aino Mutka[3] | Timo Jahnukainen[4] |
Mark Davenport[5] | Markku Heikinheimo[2,6,7] | Johanna Arola[3] |
Mikko P. Pakarinen[1,2,8]

[1]Section of Pediatric Surgery, Pediatric Liver and Gut Research Group, Children and Adolescent Department, New Children's Hospital, University of Helsinki and Helsinki University Hospital, Helsinki, Finland

[2]Pediatric Research Center, Children and Adolescent Department, New Children's Hospital, University of Helsinki and Helsinki University Hospital, Helsinki, Finland

[3]Department of Pathology, University of Helsinki and Helsinki University Hospital, Helsinki, Finland

[4]Department of Pediatric Nephrology and Transplantation, New Children's Hospital, University of Helsinki and Helsinki University Hospital, Helsinki, Finland

[5]Department of Pediatric Surgery, King's College Hospital, London, UK

[6]Department of Pediatrics, Washington University School of Medicine, St. Louis Children's Hospital, St. Louis, Missouri, USA

[7]Department of Pediatrics, Center for Child, Adolescent, and Maternal Health Research, Faculty of Medicine and Health Technology, Tampere University, Tampere, Finland

[8]Department of Women's and Children's Health, Karolinska Institute, Stockholm, Sweden

Correspondence
Iiris Nyholm, Pediatric Research Center, Children and Adolescent Department, Biomedicum 2U, Tukholmankatu 8, Helsinki 00290, Finland
Email: iiris.nyholm@helsinki.fi

Mikko P. Pakarinen, Section of Pediatric Surgery, Children and Adolescent Department, New Children's Hospital, Stenbäckinkatu 11, Helsinki 00290, Finland.
Email: mikko.pakarinen@hus.fi

Abstract

Background: We aimed to quantify ductular reaction (DR) in biliary atresia using a neural network in relation to underlying pathophysiology and prognosis.

Methods: Image-processing neural network model was applied to 259 cytokeratin-7–stained native liver biopsies of patients with biliary atresia and 43 controls. The model quantified total proportional DR (DR%) composed of portal biliary epithelium (BE%) and parenchymal intermediate hepatocytes (PIH%). The results were related to clinical data, Sirius Red–quantified liver fibrosis, serum biomarkers, and bile acids.

Results: In total, 2 biliary atresia biopsies were obtained preoperatively, 116 at Kasai portoenterostomy (KPE) and 141 during post-KPE follow-up. DR% (8.3% vs. 5.9%, $p = 0.045$) and PIH% (1.3% vs. 0.6%, $p = 0.004$) were increased at KPE in patients remaining cholestatic postoperatively. After KPE, patients with subsequent liver transplantation or death showed an increase in

- -

DR% (7.9%–9.9%, $p = 0.04$) and PIH% (1.6%–2.4%, $p = 0.009$), whereas patients with native liver survival (NLS) showed decreasing BE% (5.5%–3.0%, $p = 0.03$) and persistently low PIH% (0.9% vs. 1.3%, $p = 0.11$). In Cox regression, high DR predicted inferior NLS both at KPE [DR% (HR = 1.05, $p = 0.01$), BE% (HR = 1.05, $p = 0.03$), and PIH% (HR = 1.13, $p = 0.005$)] and during follow-up [DR% (HR = 1.08, $p < 0.0001$), BE% (HR = 1.58, $p = 0.001$), and PIH% (HR = 1.04, $p = 0.008$)]. DR% correlated with Sirius red–quantified liver fibrosis at KPE ($R = 0.47$, $p < 0.0001$) and follow-up ($R = 0.27$, $p = 0.004$). A close association between DR% and serum bile acids was observed at follow-up ($R = 0.61$, $p < 0.001$). Liver fibrosis was not prognostic for NLS at KPE (HR = 1.00, $p = 0.96$) or follow-up (HR = 1.01, $p = 0.29$).

Conclusions: DR predicted NLS in different disease stages before transplantation while associating with serum bile acids after KPE.

INTRODUCTION

Biliary atresia (BA) is a severe cholangiopathy of infancy characterized by progressive fibro-inflammatory obliteration of the biliary tree.[1] Although the first-line surgery, Kasai portoenterostomy (KPE), normalizes serum bilirubin levels by restoring the bile drainage in most cases, progression of the underlying cholangiopathy necessitates liver transplantation (LT) before adulthood in 70%–80% of the patients.[2,3] Thus, BA remains the most common indication for LT in children worldwide.[4]

Ductular reaction (DR) is a prominent feature of liver pathology in cholangiopathies such as BA.[5] In addition to compensatory bile duct proliferation, DR encompasses enhanced angiogenesis and inflammation, which together with reactive neocholangiocytes is thought to promote extracellular matrix accumulation by myofibroblasts.[6–9] DR is closely related to hepatocyte senescence and fibrogenesis in hepatobiliary injury, and blocking DR reduces liver fibrosis in preclinical studies.[10,11] The cellular origin of the newly forming bile ducts in DR is not fully established, but in addition to cholangiocyte self-proliferation, neocholangiocytes may originate from the differentiation of hepatic progenitor cells and/or transdifferentiating hepatocytes.[8] The main cellular components of DR can be visualized immunohistochemically as cytokeratin-7 (K7)-positive portal cholangiocytes and intermediate hepatocytes within the parenchyma.[8,12] Although conventional histopathology shows limited correlation with BA outcomes,[5,13] the degree of K7-positive bile duct expansion at KPE has been associated with native liver survival (NLS) and liver fibrosis in few studies with a limited number of patients,[14–17] suggesting that DR

could bear important pathophysiological implications in the progression of BA liver injury.

Emerging quantitative histopathological analyses have proved to outperform manual scoring in reproducibility and the ability to manage complex features of various diseases and tissues.[18–20] A recently published image-processing neural network of K7-stained liver sections developed for primary sclerosing cholangitis showed improved performance in identifying various DR components with accuracy beyond the reach of manual scoring and enhanced prognostic value.[21,22]

Here, we aimed to address the prognostic and pathophysiological significance of DR in BA by developing and applying a histopathological neural network model to a large cohort of native liver biopsies obtained over different disease stages, at KPE and during postoperative follow-up until LT. Model components were related to essential outcome variables and to explanatory factors including serum liver biochemistry, bile acids, and novel biomarkers previously shown to associate the progression of DR in a limited series of BA.[23–25]

METHODS

Patients and liver biopsies

All patients with BA with available native liver biopsy specimens obtained at KPE (n = 63) and/or postoperative follow-up (n = 76) during 1990–2020 in Helsinki University Hospital (Finland) or at KPE (n = 53) during 2005–2012 in King's College Hospital (London, UK) were included (Figure 1). After excluding unrepresentative and poor-quality specimens, the study population consisted of 136
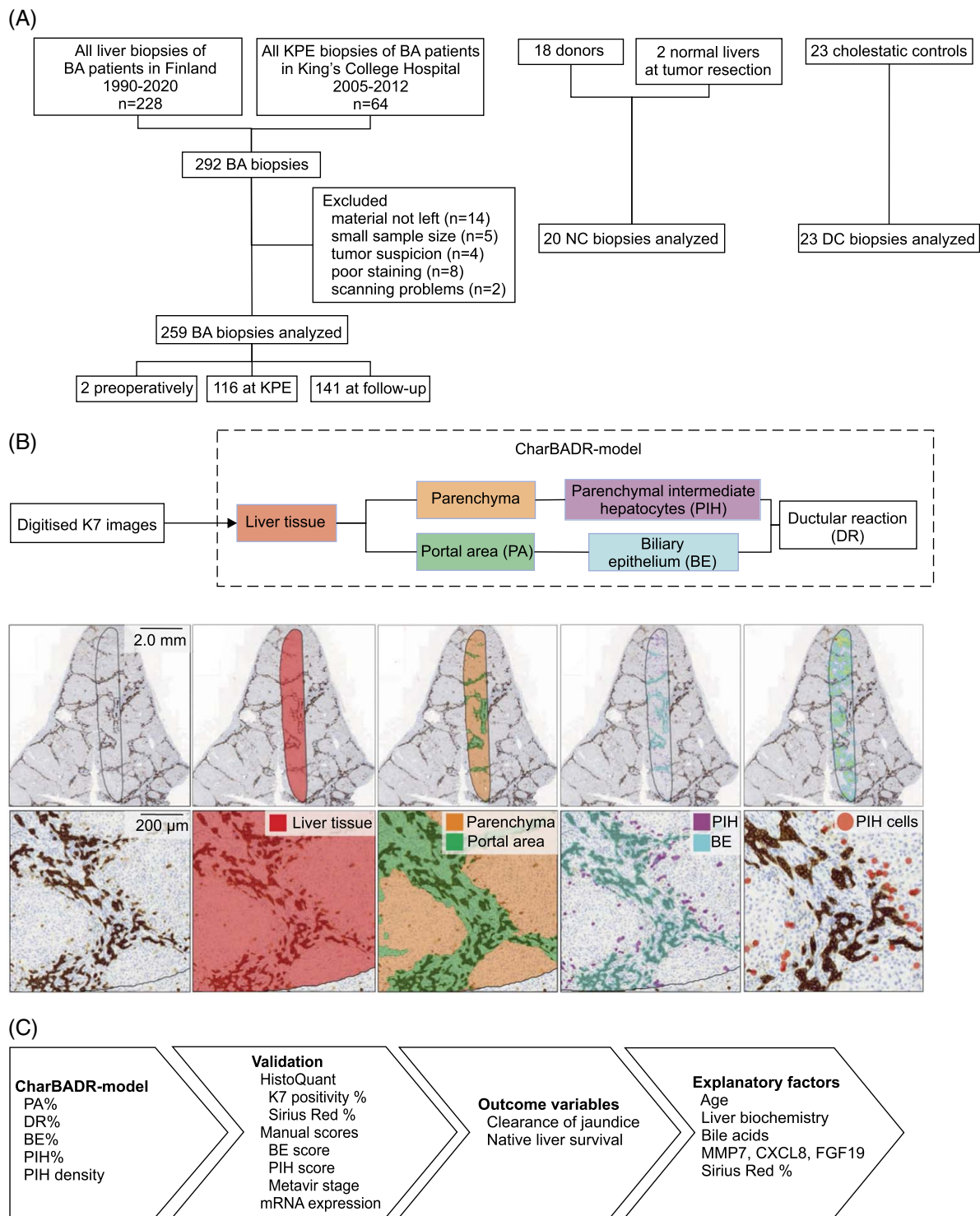
FIGURE 1 Study design and CharBADR model. (A) Flowchart of enrolled and excluded biopsies of patients with BA and controls. (B) CharBADR model was applied to 302 scanned images. The first layer identified liver tissue (red) and the second layer segmented the liver tissue into parenchyma (orange) and portal area (green). K7-positive areas were identified, and areas located in parenchyma were classified as parenchymal intermediate hepatocytes (purple) and areas located in portal areas as biliary epithelium (blue). Finally, individual parenchymal intermediate hepatocytes (circled red) were identified and calculated. (C) CharBADR results were validated with HistoQuant proportional areas, manual scores, and liver *KRT7* expression, compared to clinical outcome variables and explanatory factors. Abbreviations: BA, biliary atresia; CharBADR, CHARacterization of Biliary Atresia–related Ductular Reaction; CXCL8, cysteine-X cysteine motif chemocine ligand 8; DC, disease control; KPE, Kasai portoenterostomy; MMP7, matrix metalloproteinase 7; NC, normal control.

patients with BA with 259 native liver biopsies obtained preoperatively (n = 2), at KPE (n = 116), during protocol post-KPE follow-up (n = 103), or at LT (n = 38) (Figure 1). According to the national protocol in Finland, percutaneous core needle liver biopsies are performed with ultrasound guidance under general anesthesia for endoscopic variceal surveillance routinely at 5-year intervals starting 1 year after KPE in addition to liver biopsies obtained at KPE and LT.[14] Medical records were retrospectively assessed for clinical data and serum liver biochemistry. Clearance of jaundice (COJ) was defined as the decrease of serum bilirubin below 20 µmol/L following KPE.

Cholestatic and normal controls

Liver biopsies obtained at a median age of 64 (41–2276) days from children with other cholestatic disorders (n = 23) were included as disease controls (Supplemental Table S1, http://links.lww.com/HC9/A676). Biopsies obtained from healthy liver parenchyma during local mesenchymal hamartoma or hepatoblastoma resection (n = 2) or pediatric liver donors (n = 18) at median age 8.1 (2–13.8) years were used as normal controls (Figure 1).

Quantitative CHARacterization of Biliary Atresia–related Ductular Reaction model

K7 immunohistochemistry was performed automatically, and digitized images were uploaded to Aiforia Cloud (Aiforia Technologies), a commercial platform designed for automated histological image analysis, where CharBADR (CHARacterization of Biliary Atresia–related Ductular Reaction) model was applied to all images (Figure 1).

CharBADR consists of independent nested convolutional neural networks trained by a pathologist based on a previously developed quantitative neural network model for the analysis of DR in primary sclerosing cholangitis.[21] The first convolutional neural network defines intact liver tissue, and the second one segments portal areas (PAs) and the liver parenchyma. The third convolutional neural network identifies biliary epithelium (BE) and the fourth one parenchymal intermediate hepatocytes (PIH) based on K7 positivity of the portal and parenchymal areas, respectively (Figure 1, Supplemental Figure S1, http://links.lww.com/HC9/A677, Supplemental Table S2, http://links.lww.com/HC9/A676). PA and BE were expressed in relation to the liver tissue area resulting in proportional PA (PA%) and biliary epithelium (BE%), which includes portal cholangiocytes of original and reactive proliferating bile ducts. PIH area and cells were related to the parenchymal area to calculate proportional PIH area (PIH%) and parenchymal intermediate hepatocyte density as number of cells/mm² (PIHD). The total K7-positive area,

composed of BE and PIH, was related to the entire liver tissue area to assess the overall proportional area of DR (DR%) (Supplemental Figure S2, http://links.lww.com/HC9/A678). For further details, see Supplemental Methods, http://links.lww.com/HC9/A676.

Conventional assessment of DR and liver fibrosis

K7-positive bile duct proliferation corresponding BE% and parenchymal hepatocytes corresponding PIH% were manually scored, and proportional K7-positive area in liver specimens was quantified using Case-Viewer HistoQuant software. Liver fibrosis was assessed by Metavir staging and by measuring proportional Sirius Red positive area using HistoQuant. Further details are provided in the Supplemental Methods, http://links.lww.com/HC9/A676.

Serum biomarkers and bile acids

Serum concentrations (n = 152) of FGF19, cysteine-X cysteine motif chemokine ligand 8, and matrix metalloproteinase 7 were measured using ELISA. Serum total and individual bile acids including conjugated and unconjugated bile acids (n = 88) were quantified by gas-liquid chromatography. For further details, see Supplemental Methods, http://links.lww.com/HC9/A676.

Liver mRNA expression analyses

mRNA expression of liver biopsies (n = 129) was measured by quantitative real-time PCR. Expression levels were calculated using the ΔΔCt method. For further details, see Supplemental Methods, http://links.lww.com/HC9/A676.

Statistical analysis

RStudio (R version 4.0.3) was used for data analysis. All continuous variables are expressed as medians and interquartile ranges. Cross-sectional validation between model parameters and conventional histopathological assessments of the biopsy specimens of patients with BA and controls were performed with root mean squared error analyses and Spearman rank correlations. Case-control analyses of patients with BA and controls and BA subgroups were analyzed with nonparametric Mann-Whitney *U* tests. In comparisons between KPE and post-KPE biopsies, one biopsy at KPE and the first follow-up biopsy of each patient were included and analyzed with Wilcoxon signed rank tests. Correlations of model parameters with liver

biochemistry or serum biomarkers of patients with BA were analyzed cross-sectionally using Spearman rank correlations.

Survival analyses were performed with time-dependent univariable Cox proportional hazards regression models using continuous variables. Survival start time was defined as the date of birth in the KPE cohort and the date of the index biopsy in the follow-up cohort. Stop time was the primary event or the latest follow-up appointment in the KPE cohort. Due to repeated biopsies in the follow-up cohort, stop time was defined as the date of the next follow-up biopsy from the index biopsy, primary event, or latest follow-up appointment if the index biopsy was the last one obtained. Multivariable mixed effects time-dependent Cox regression model was performed with continuous variables and included CharBADR components, HistoQuant Sirius Red, COJ, and gamma glutamyl transferase (GGT), and was adjusted with year of acquisition and time after KPE. Variables for multivariable models were selected based on previous literature.[13] The primary outcome event was defined as LT or death, and survival time was measured in a maximum of 10 years. Survival data were visualized graphically with Kaplan-Meier curves using dichotomic cutoffs. Wald and log-rank tests choosing the least significant method were used for statistical comparisons of the survival curves. Optimal cutoffs were selected with receiver operating characteristics analysis based on the maximum sum of dynamic specificity and cumulative sensitivity for the primary event in a maximum of 10 years after the index biopsy. p values less than 0.05 were considered statistically significant.

Ethics

The study was approved by the Research Ethics Committee (345/13/03/03/2008) and Review Board (§70HUS/284/2019) of Helsinki University Hospital and by the National Health Service Research Ethics Committee in the United Kingdom (12/WA/0282 and 18/SC/0058). The study protocol conforms to the guidelines of the Declaration of Helsinki and Istanbul. An informed consent for use of samples in research was obtained from patients or patients' legal guardians.

RESULTS

Clinical patient characteristics

Of the 136 patients with BA, 58% normalized their bilirubin following KPE. Two-year, 5-year, and overall NLS was 56%, 48%, and 38%, respectively. Follow-up biopsies were obtained at a median of 4.58 (1.63–9.70) years of age. Clinical patient characteristics at the time of liver biopsy are presented in Table 1.

Validation and relation to conventional assessments

In CharBADR model, proportional amount of BE (BE%) ($R = 0.67$, $p < 0.001$, root mean squared error = 1.10) and parenchymal intermediate hepatocytes (PIH%) ($R = 0.87$, $p < 0.001$, root mean squared error = 1.62) showed similarity with respective manual scorings, and overall ductular reaction (DR%) of CharBADR paralleled the overall proportional K7 positivity using HistoQuant ($R = 0.93$, $p < 0.001$). All CharBADR biliary components (DR%, BE%, PIH%, and PIHD) positively correlated with liver *KRT7* mRNA expression (Supplemental Figure S3, http://links.lww.com/HC9/A679, Supplemental Table S3, http://links.lww.com/HC9/A676). PA%, reflecting portal fibrogenesis–associated portal tract expansion, correlated with Metavir fibrosis stage ($R = 0.56$, $p < 0.001$) and proportional Sirius Red fibrosis area ($R = 0.64$, $p < 0.001$) (Supplemental Figure S3, http://links.lww.com/HC9/A679). CharBADR biliary components, PA%, and *KRT7* expression were increased in BA biopsies compared to cholestatic and normal control biopsies (Supplemental Figure S2, http://links.lww.com/HC9/A678).

CharBADR predicted KPE outcomes

At KPE, DR%, PIH%, and PIHD were increased among patients who did not clear their jaundice compared to patients normalizing their bilirubin after KPE (Figure 2). The difference in BE% did not reach statistical significance.

In univariable Cox regression models, all CharBADR biliary components were highly predictive for inferior NLS (Supplemental Table 4, http://links.lww.com/HC9/A676), whereas PA%, Metavir fibrosis stage [HR: 1.24 (95% CI: 0.94–1.64), $p = 0.14$], and Sirius Red quantification [HR: 1.00 (95% CI: 0.97–1.04), $p = 0.96$] were not (Supplemental Table S4, http://links.lww.com/HC9/A676). When CharBADR biliary components were dichotomized with optimal cutoffs, patients with higher values showed decreased cumulative NLS (Figure 2, Supplemental Table S5, http://links.lww.com/HC9/A676). The decrease in cumulative NLS was most prominent for higher DR% and BE% and centered around 2 years following KPE. Accordingly, DR% was lower at KPE among patients who were surviving with their native livers at 2 years, but not at 5 years (Figure 3).

CharBADR associated with age and liver injury at KPE

At KPE, patients with cystic BA showed lower BE% [3.6% (2.7–4.7)] than those with noncystic BA [6.1% (3.5–9.2), $p = 0.04$]. CharBADR biliary components

TABLE 1 Clinical characteristics, serum liver biochemistry, and conventional liver histopathology of patients with BA according to the timing of liver biopsy

	All patients	At KPE	Post-KPE
Patients, n[a]	136	116	76
Liver biopsies, n	259	116	141
Place of care, n (%)			
Helsinki, Finland	83 (61)	63 (54)	76 (100)
London, UK	53 (39)	53 (46)	0 (0)
Male, n (%)	59 (43)	51 (44)	36 (47)
Type of BA, n (%)			
1 or 2	7 (5)	5 (4)	7 (9)
3	126 (93)	111 (96)	66 (90)
Unclear	3 (2)	0 (0)	3 (4)
Cystic disease, n (%)[b]	16 (12)	16 (14)	8 (11)
Splenic malformation, n (%)	18 (13)	14 (12)	10 (13)
Isolated disease, n (%)	102 (75)	88 (76)	53 (70)
Age at KPE, d	64 (41–84)	64 (41–84)	63 (41–85)
Clearance of jaundice, n (%)[c]	77 (58)	66 (59)	50 (67)
Outcome, n (%)			
Native liver	51 (38)	44 (38)	35 (46)
Died with native liver	6 (4)	6 (5)	1 (1)
LT	72 (53)	64 (55)	33 (43)
Died after LT	7 (5)	2 (2)	7 (9)
Native liver survival, y	3.27 (0.99–8.52)	3.54 (0.99–8.29)	5.14 (1.40–11.89)
2-year native liver survival, n (%, 95% CI)[d]	76 (56, 48–65)	66 (57, 48–66)	47 (62, 50–73)
5-year native liver survival, n (%, 95% CI)[d]	65 (48, 40–57)	55 (48, 38–57)	46 (61, 49–71)
Age at liver transplantation, y	1.44 (0.84–2.82)	1.37 (0.84–2.51)	1.45 (0.85–5.50)
Liver biochemistry at biopsy			
Bilirubin, μmol/L	99 (12–168)	153 (125–195)	13 (7–51)
Conjugated bilirubin, μmol/L	58 (5–123)	117 (94–144)	7 (3–33)
ALT, U/L	83 (40–140)	121 (82–198)	57 (30–113)
AST, U/L	127 (66–226)	201 (122–284)	87 (51–153)
GGT, U/L	167 (52–452)	432 (230–804)	60 (28–154)
APRI	1.15 (0.57–2.13)	0.91 (0.55–1.59)	1.42 (0.59–2.28)
Liver histopathology			
BE score, 0–2	2 (1–2)	2 (1–2)	1 (1–2)
PIH score, 0–4	2 (1–3)	1 (1–2)	2 (1–3)
HistoQuant K7 positivity, %	5.29 (2.91–10.57)	5.70 (3.45–9.02)	4.96 (2.34–11.79)
Metavir fibrosis stage, 0–4	3 (2–4)	3 (2–3)	4 (2–4)
HistoQuant Sirius Red, %	14.87 (8.76–26.02)	10.48 (8.08–17.11)	20.59 (14.11–31.32)

Note: Reference value for bilirubin <20 μmol/L, conjugated bilirubin 0–5 μmol/L, ALT <40 U/L, AST <50 U/L, and GGT <50 U/L.
[a]Fifty-six patients had biopsies obtained both at KPE and post-KPE follow-up and 32 patients had repeated post-KPE follow-up biopsies. Data are presented as median with interquartile range or frequencies.
[b]Information of 5 patients was not available.
[c]Information of 4 patients was not available.
[d]Information of 1 patient was not available.
Abbreviations: ALT, alanine aminotransferase; APRI, AST to platelet ratio index; AST, aspartate transaminase; BA, biliary atresia; BE, biliary epithelium; GGT, gamma glutamyl transferase; KPE, Kasai portoenterostomy; LT, liver transplantation; PIH, parenchymal intermediate hepatocyte.

correlated positively with KPE age, serum FGF19, Sirius Red–quantified fibrosis, and serum liver biochemistry values other than GGT (Supplemental Figure S4, http://links.lww.com/HC9/A680, Supplemental Table S6, http://links.lww.com/HC9/A676). BE% ($R = 0.47$, $p < 0.001$)

and DR% ($R = 0.43$, $p < 0.001$) also correlated with the Metavir fibrosis stage. Serum bile acids had no meaningful associations with CharBADR components at KPE (Supplemental Table S6, http://links.lww.com/HC9/A676).
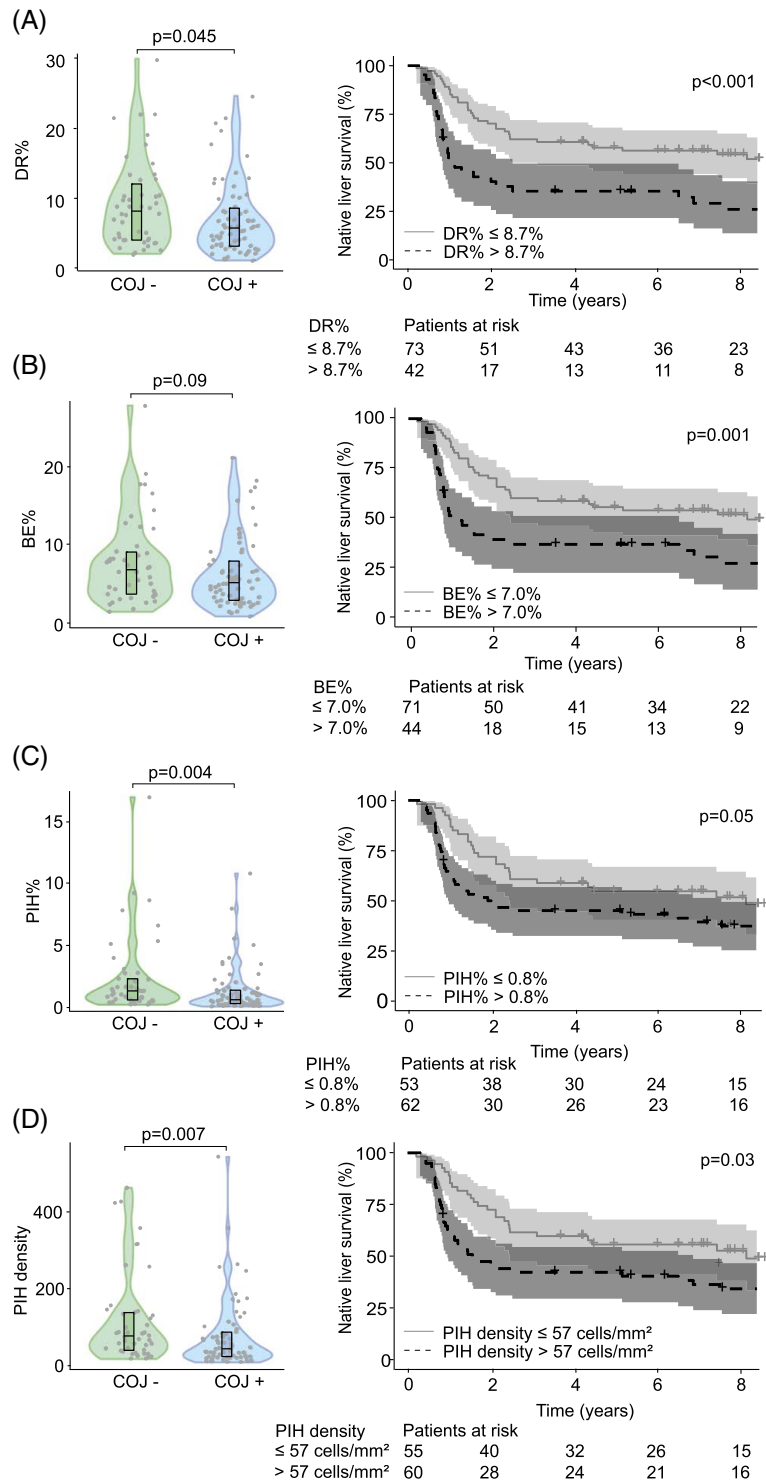
FIGURE 2 DR at KPE was increased in patients with inferior short-term and long-term outcomes. (A) DR%, (B) BE%, (C) PIH%, and (D) PIH density of KPE biopsy specimens according to COJ and Kaplan-Meier native liver survival curves according to optimal cutoffs at KPE (n = 115). Optimal cutoffs were selected with receiver operating characteristics analysis based on the maximum sum of specificity and sensitivity. Violin plots display median, interquartile range, and individual data points. The shaded areas of Kaplan-Meier curves represent 95% CI. Abbreviations: BE, biliary epithelium; COJ, clearance of jaundice; DR, ductular reaction; KPE, Kasai portoenterostomy; PIH, parenchymal intermediate hepatocyte.
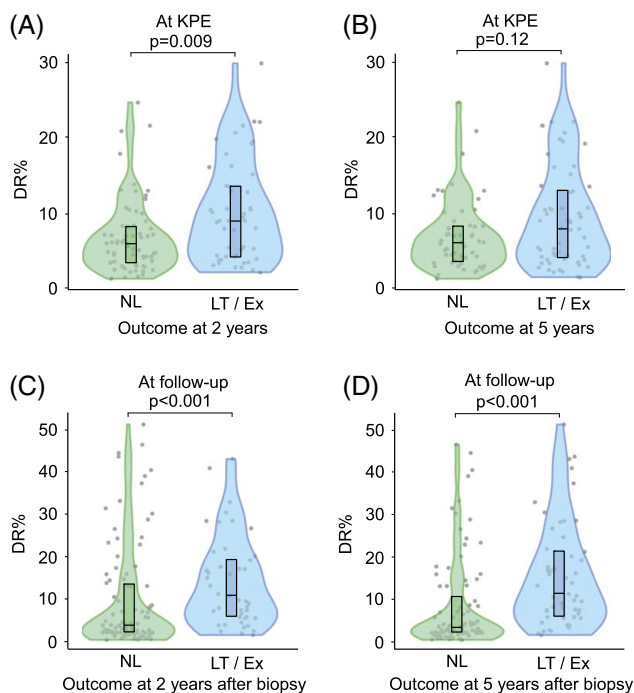
FIGURE 3 Association of DR in liver biopsies obtained at KPE and follow-up with subsequent 2-year and 5-year native liver survival. DR% according to outcome at (A) 2 years, (B) 5 years after KPE, (C) 2 years, and (D) 5 years after follow-up biopsy. Abbreviations: DR, ductular reaction; Ex, exitus; KPE, Kasai portoenterostomy; LT, liver transplantation; NL, native liver.

CharBADR in post-KPE follow-up biopsies predicted NLS

In univariable Cox regressions, high DR%, BE%, and PIH% in follow-up biopsy specimens predicted inferior NLS (Supplemental Table S7, http://links.lww.com/HC9/A676, Supplemental Table S8, http://links.lww.com/HC9/A676). Interestingly, PA%, Metavir stage [HR: 1.17 (95% CI: 0.61–2.21), $p = 0.63$], or Sirius Red–quantified fibrosis [HR: 1.00 (95% CI: 0.96–1.05), $p = 0.91$] were not predictive for NLS at follow-up (Supplemental Table S7, http://links.lww.com/HC9/A676). The prognostic abilities of DR% and PIH% maintained in a multivariable model including COJ, Sirius Red–quantified liver fibrosis, and GGT adjusted with the year of acquisition and time after KPE (Supplemental Table S9, http://links.lww.com/HC9/A676).

In follow-up biopsy specimens, DR%, PIH%, and PIHD remained markedly increased during the follow-up period in different age groups of patients who eventually received LT compared to native liver survivors (Figure 4). The differences were not as significant for BE%, which reduced distinctly beyond 2 years after KPE in both groups. When NLS after each follow-up biopsy was assessed with dichotomized optimal cutoffs, patients with higher CharBADR biliary components showed markedly decreased subsequent cumulative post-biopsy NLS (Figure 4). These findings remained similar when

specimens obtained at the time of LT were removed from the analyses (Supplemental Figure S5, http://links.lww.com/HC9/A681). Importantly, the negative prognostic ability of CharBADR persisted throughout the follow-up as the NLS curves for DR%, BE%, PIH%, and PIHD progressively diverted from each other, and absolute differences in DR%, PIH%, and PIHD between native liver survivors (NLS) and transplanted patients grew more distinct during follow-up (Figure 4). Follow-up DR% was lower among patients who normalized their serum bilirubin after KPE (Figure 5), and among those who were surviving with their native livers both at 2 years and at 5 years after the index biopsy (Figure 3).

When only patients with both KPE and at least one follow-up biopsy were included (n = 56), BE% decreased and PIH% increased in post-KPE follow-up specimens (Figure 5). Patients with a primary event during follow-up (n = 28) showed a prominent increase in DR% from 7.9% (4.3–11.4) to 9.9% (6.0–17.1; $p = 0.04$) and PIH% from 1.6% (0.7–2.7) to 2.4% (1.2–11.4; $p = 0.009$), whereas BE% decreased from 5.5% (3.2–6.6) to 3.0% (2.2–5.5; $p = 0.03$) and PIH% remained low [0.9% (0.5–1.5) vs. 1.3% (0.1–5.0), $p = 0.11$] among native liver survivors (Figure 5).

CharBADR correlated with serum bile acids and liver fibrosis at post-KPE follow-up

CharBADR biliary components correlated negatively with age at biopsy and positively with serum bile acids and liver biochemistry values including GGT and serum cysteine-X cysteine motif chemocine ligand 8 and matrix metalloproteinase 7, but not with FGF19 (Figure 6, Supplemental Table S10, http://links.lww.com/HC9/A676). CharBADR components were also positively correlated with Metavir fibrosis stage [DR% (R = 0.59, $p < 0.001$), BE% (R = 0.52, $p < 0.001$), PIH% (R = 0.53, $p < 0.001$), and PIHD (R = 0.52, $p < 0.001$)] and with Sirius Red quantification (Supplemental Table S10, http://links.lww.com/HC9/A676).

At post-KPE follow-up, all CharBADR biliary components correlated strongly with serum total primary bile acids, as well as cholic and chenodeoxycholic acids individually. These correlations were most pronounced for PIH% and PIHD (Figure 6, Supplemental Table S10). The concentration of ursodeoxycholic acid (UDCA) was highest among individual serum bile acids, likely caused by UDCA treatment in 72 (95%) patients during follow-up. Like primary bile acids, UDCA was highly correlated with all CharBADR biliary components, being the most abundant bile acid in patients with extensive PIH% at follow-up (Figure 6, Supplemental Table S10, http://links.lww.com/HC9/A676). Still, when including all bile acids except for UDCA, positive correlations with PIH% (R = 0.66, $p < 0.001$), PIHD (R = 0.66, $p < 0.001$), BE% (R = 0.42, $p = 0.002$), and DR% (R = 0.59, $p < 0.001$) were
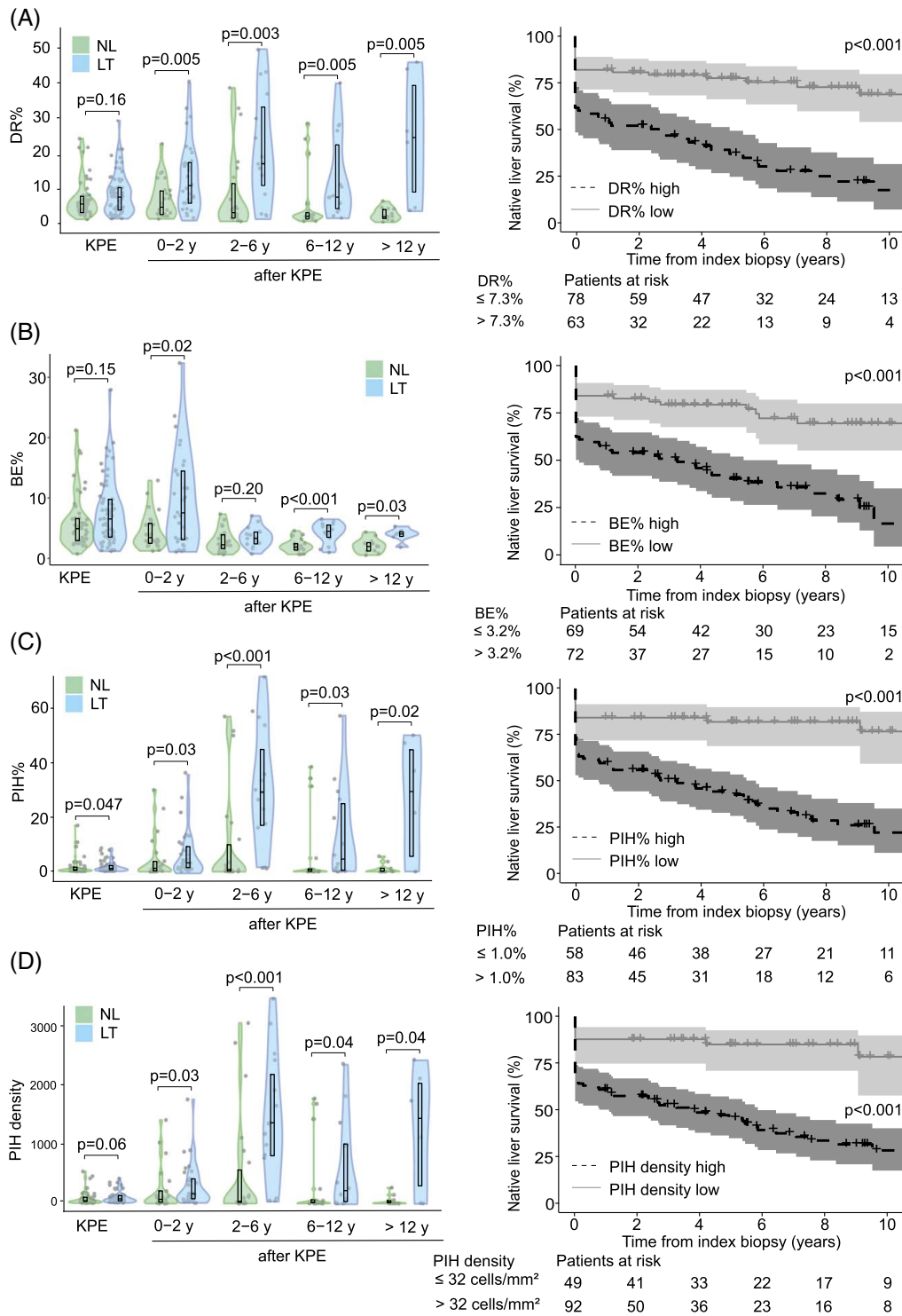
FIGURE 4 DR persisted and predicted decreased native liver survival during follow-up. (A) DR%, (B) BE%, (C) PIH%, and (D) PIH density in patients with follow-up biopsies at KPE and during follow-up according to age [KPE (n = 116); 0–2 y (n = 55); 2–6 y (n = 37); 6–12 y (n = 32); > 12 y (n = 17)] and subsequent LT or NL survival at latest follow-up, and Kaplan-Meier native liver survival curves according to optimal cut points calculated with receiver operator characteristics analyses. The median time from protocol follow-up biopsy to LT was 4.3 (2.4–6.6) years. Violin plots display median, interquartile range, and individual data points. The shaded areas of Kaplan-Meier curves represent 95% CI. Abbreviations: BE, biliary epithelium; DR, ductular reaction; KPE, Kasai portoenterostomy; LT, liver transplantation; NL, native liver; PIH, parenchymal intermediate hepatocyte.

maintained. No associations of CharBADR components with other secondary bile acids, deoxycholic or lithocholic acids, were observed. At post-KPE follow-up, serum total and all individual bile acids, except deoxycholic acid, were predictive for NLS in univariable Cox regression models (Supplemental Table S11, http://links.lww.com/HC9/A676).
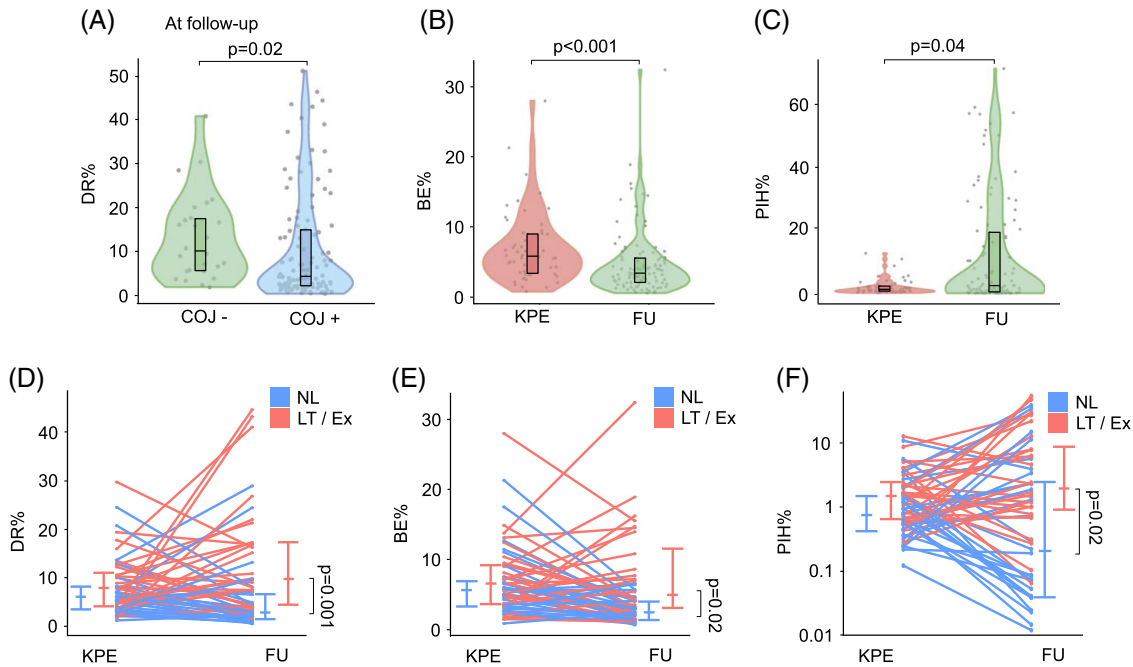
FIGURE 5   BE decreased and PIH increased after KPE. (A) DR% in follow-up liver specimens according to COJ. Changes in (B) BE% and (C) PIH% after KPE in patients with both KPE and follow-up biopsy. Changes in (D) DR%, (E) BE%, and (F) PIH% in individual patients after KPE according to native liver survival. Violin plots display median, interquartile range, and individual data points. Abbreviations: BE, biliary epithelium; COJ, clearance of jaundice; DR, ductular reaction; Ex, exitus; FU, follow-up; KPE, Kasai portoenterostomy; LT, liver transplantation; NL, native liver; PIH, parenchymal intermediate hepatocyte.

DISCUSSION

In the present study, we assessed DR by applying a novel histopathological neural network to 259 K7-stained liver biopsy specimens in patients with BA. At KPE, prominent DR was associated with failure to resolve cholestasis and, unlike liver fibrosis, predicted decreased NLS. While PIHs became the prevailing element of DR in native liver survivors after KPE, the predictive ability of DR was sustained in follow-up liver specimens. During post-KPE follow-up, DR was closely correlated with serum bile acids, emphasizing the potential role of accumulated bile acids promoting DR after KPE.[26,27]

In accordance with our findings, high DR at KPE, assessed with manual scorings or conventional computer-aided methods, has been associated with decreased COJ rate and NLS in studies with a limited number of patients and follow-up.[15,16] Here, the robust prognostic effect of DR for NLS at KPE was mainly underpinned by the expansion of BE (BE%) by proliferating bile ducts and it lasted for around 2 years until the survival curves paralleled. In line with these findings, BE% abruptly decreased in follow-up biopsy specimens obtained beyond 2 years after KPE, demonstrating that patients with persisting extensive bile duct proliferation had required LT by that time. Moreover, in patients with liver biopsies obtained both at the time and after KPE, BE% decreased among those who continued to survive with their native livers. Although liver fibrosis was not predictive for NLS at KPE, it was associated with DR in line with previous studies in BA[14,15,28,29] and various adult liver diseases.[8,11,21,30–32] Associations of CharBADR biliary components with KPE age and serum liver biochemistry as well as lower BE% in patients with cystic BA further support the central role of DR in BA liver injury. A younger KPE age and cystic BA are established positive prognosticators for NLS.[3,33]

In the present study, we showed for the first time that high DR also at post-KPE follow-up predicted subsequent NLS, while PIHs became the dominant constituent of DR and largely replaced BE (BE%) in patients who survived with their native liver beyond 2 years. Although successful KPE modified the main features of DR, it maintained its close associations with liver fibrosis and biochemical markers of liver injury. Previously, excessive DR has been associated with the progression of various adult liver diseases, such as the occurrence of steatohepatitis in NAFLD and decompensation in hepatitis C cirrhosis.[34,35] Other studies have reported DR to be associated with higher MELD scores in alcoholic hepatitis and high alkaline phosphatase levels in primary biliary cholangitis.[32,36] DR also predicted the development of cholangiocarcinoma and liver-related death in primary sclerosing cholangitis[22] as well as overall survival in patients with hepatitis C cirrhosis and alcoholic hepatitis.[34,37]
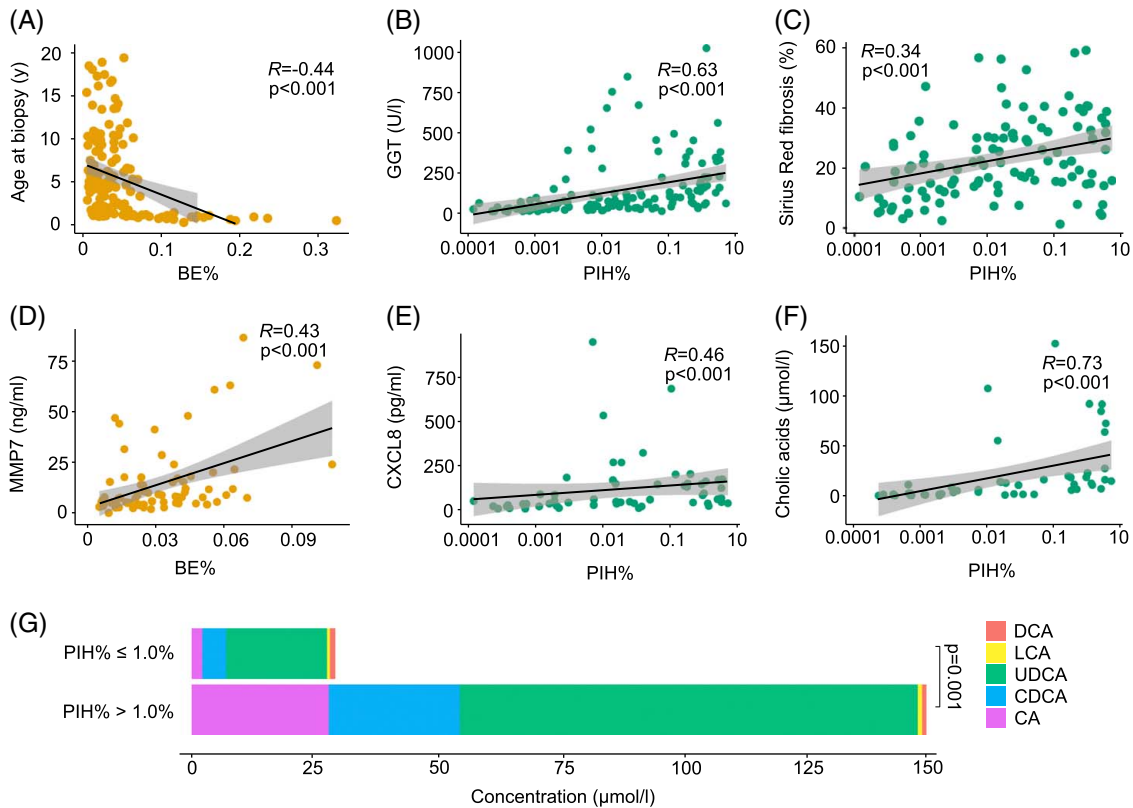
FIGURE 6 DR associated with serum bile acids and other explanatory factors at follow-up. Spearman rank correlations of (A) BE% and age at biopsy, (B) PIH% and GGT, (C) PIH% and proportional Sirius Red fibrosis area, (D) BE% and MMP7, (E) PIH% and CXCL8, and (F) PIH% and cholic acids at follow-up. (G) Combined conjugated and unconjugated serum total bile acids and proportions of individual bile acids according to the optimal cutoff of PIH% for native liver survival. The shaded areas represent 95% CI. Abbreviations: BE, biliary epithelium; CA, cholic acid; CDCA, cheno-deoxycholic acid; CXCL8, cysteine-X cysteine motif chemocine ligand 8; DCA, deoxycholic acids; DR, ductular reaction; GGT, gamma glutamyl transferase; LCA, lithocholic acid; MMP7, matrix metalloproteinase 7; PIH, parenchymal intermediate hepatocyte; UDCA, ursodeoxycholic acid.

Although DR's link to the progression of liver injury is indisputable, the underlying mechanisms of DR remain unclear in patients with BA.[38–43] In preclinical models mimicking BA, blocking Notch signaling decreases cytokeratin-19 expression suggesting that DR arises from hepatic progenitor cells or transdifferentiating hepatocytes instead of self-proliferating cholangiocytes.[8,38,44] In line with this, PIHs, rather than BE, were increased in follow-up specimens among patients requiring subsequent LT. In addition, serum bile acid levels were tightly correlated with CharBADR biliary components after KPE, especially cholic acid with PIHs. Accumulated taurocholate has been shown to induce biliary differentiation of progenitor cells in DR as well as cholangiocyte proliferation,[26,27] suggesting that bile acids may have contributed to biliary transformation of hepatocytes (PIH). In line with our findings, a recent study linked high total serum bile acids measured at 6 months after successful KPE to decreased NLS and development of portal hypertension.[45] In another study, serum FGF19 measured at KPE predicted NLS with an association with DR.[25] Herein, CharBADR biliary components showed positive correlations with serum FGF19 at KPE, but not at post-KPE follow-up. While reasons for these reversed associations of FGF19 and bile acids require further investigations, they indicate differential regulation of DR in different stages of BA. Accordingly, serum matrix metalloproteinase 7 and cysteine-X cysteine motif chemocine ligand 8, which have been previously connected with the progression of DR following KPE,[25,26] showed more uniform and stronger correlations with CharBADR components during follow-up than at KPE.

Despite being one of the largest native liver biopsy materials in BA reported thus far, and the first one to address DR after KPE, one limitation of our study is that serial biopsies obtained at the time and after KPE were not available for all patients. To control the variable number and timing of follow-up biopsies due to clinical constraints, patients were grouped into different age groups, and post-biopsy NLS was analyzed with time-dependent models. Only KPE biopsy specimens were available from the other center, although previously reported surgical and medical approaches and outcomes were comparable between the participating units.[14,46] Uniform cohorts predispose statistical thresholds to bias, hence the results should be validated with an independent series of BA biopsies in the future. We only analyzed serum

total concentrations of bile acids, but previous studies have confirmed that serum bile acids are exclusively conjugated in patients with BA both at and after successful KPE.[45,47] Also, some variability in the timing of immunohistochemistry and scanning of cut sections may have predisposed automated analysis to unexpected analytical inaccuracies. However, the main strengths of neural network image analysis include the lack of inter- and intraobserver human variability and the ability to quantify validated continuous variables.

All in all, our findings demonstrate a central role for DR in predicting outcomes of KPE that surpassed liver fibrosis. Although DR at KPE was dominated by the expansion of BE with correlation to FGF19, PIHs became the prevailing DR element among long-term native liver survivors with a close association to accumulated serum bile acids. Further understanding of differential regulation and the contribution of the bile acids-FGF19 axis to DR at different stages of BA is important for the development of efficient therapeutic approaches.

AUTHOR CONTRIBUTIONS

Supervision, study concept: Mikko P. Pakarinen. Data analysis and interpretation, manuscript draft: Iiris Nyholm and Mikko P. Pakarinen. Developing the model: Nelli Sjöblom and Johanna Arola. Data acquisition, revision, and final approval of the submitted article: all authors.

FUNDING INFORMATION

CONFLICTS OF INTEREST

ORCID

Iiris Nyholm https://orcid.org/0000–0003–4999–4280
Nelli Sjöblom https://orcid.org/0000–0002–3360–6645
Marjut Pihlajoki https://orcid.org/0000–0002–9869–5706
Maria Hukkinen https://orcid.org/0000–0002–2622–8391
Aino Mutka https://orcid.org/0000–0002–2885–3211
Timo Jahnukainen https://orcid.org/0000–0002–1815–7327
Mark Davenport https://orcid.org/0000–0002–0938–2717
Markku Heikinheimo https://orcid.org/0000–0001–9452–0661
Johanna Arola https://orcid.org/0000–0003–3865–5507
Mikko P. Pakarinen https://orcid.org/0000–0001–6016–6334

REFERENCES

1. Hartley JL, Davenport M, Kelly DA. Biliary atresia. Lancet. 2009; 374:1704–13.
2. Kasai M, Kimura S, Asakura Y, Suzuki H, Taira Y, Ohashi E. Surgical treatment of biliary atresia. J Pediatr Surg. 1968;3:665–75.
3. Hukkinen M, Ruuska S, Pihlajoki M, Kyrönlahti A, Pakarinen MP. Long-term outcomes of biliary atresia patients surviving with their native livers. Best Pract Res Clin Gastroenterol. 2022;56–57:101764.
4. de Ville de Goyet J, Baumann U, Karam V, Adam R, Nadalin S, Heaton N, et al. European Liver Transplant Registry: Donor and transplant surgery aspects of 16,641 liver transplantations in children. Hepatology. 2022;75:634–45.
5. Russo P, Magee JC, Anders RA, Bove KE, Chung C, Cummings OW, et al. Key histopathologic features of liver biopsies that distinguish biliary atresia from other causes of infantile cholestasis and their correlation with outcome: A multicenter study. Am J Surg Pathol. 2016;40:1601–15.
6. Roskams TA, Theise ND, Balabaud C, Bhagat G, Bhathal PS, Bioulac-Sage P, et al. Nomenclature of the finer branches of the biliary tree: Canals, ductules, and ductular reactions in human livers. Hepatology. 2004;39:1739–45.
7. Gouw ASH, van den Heuvel MC, Boot M, Slooff MJH, Poppema S, de Jong KP. Dynamics of the vascular profile of the finer branches of the biliary tree in normal and diseased human livers. J Hepatol. 2006;45:393–400.
8. Sato K, Marzioni M, Meng F, Francis H, Glaser S, Alpini G. Ductular reaction in liver diseases: Pathological mechanisms and translational significances. Hepatology. 2019;69:420–30.
9. Fabris L, Brivio S, Cadamuro M, Strazzabosco M. Revisiting epithelial-to-mesenchymal transition in liver fibrosis: Clues for a better understanding of the "reactive" biliary epithelial phenotype. Stem Cells Int. 2016;2016:2953727.
10. Wu N, Meng F, Invernizzi P, Bernuzzi F, Venter J, Standeford H, et al. The secretin/secretin receptor axis modulates liver fibrosis through changes in transforming growth factor-β1 biliary secretion in mice. Hepatology. 2016;64:865–79.
11. Richardson MM, Jonsson JR, Powell EE, Brunt EM, Neuschwander–Tetri BA, Bhathal PS, et al. Progressive fibrosis in nonalcoholic steatohepatitis: Association with altered regeneration and a ductular reaction. Gastroenterology. 2007;133:80–90.
12. Gouw ASH, Clouston AD, Theise ND. Ductular reactions in human liver: Diversity at the interface. Hepatology. 2011;54:1853–63.
13. Hukkinen M, Pihlajoki M, Pakarinen MP. Predicting native liver injury and survival in biliary atresia. Semin Pediatr Surg. 2020;29:150943.
14. Hukkinen M, Kerola A, Lohi J, Heikkilä P, Merras-Salmio L, Jahnukainen T, et al. Treatment policy and liver histopathology predict biliary atresia outcomes: Results after national centralization and protocol biopsies. J Am Coll Surg. 2018;226:46–57.
15. Santos JL, Kieling CO, Meurer L, Vieira S, Ferreira CT, Lorentz A, et al. The extent of biliary proliferation in liver biopsies from

patients with biliary atresia at portoenterostomy is associated with the postoperative prognosis. J Pediatr Surg. 2009;44:695–701.

16. Kinugasa Y, Nakashima Y, Matsuo S, Shono K, Suita S, Sueishi K. Bile ductular proliferation as a prognostic factor in biliary atresia: An immunohistochemical assessment. J Pediatr Surg. 1999;34:1715–20.

17. Luo Z, Shivakumar P, Mourya R, Gutta S, Bezerra JA. Gene expression signatures associated with survival times of pediatric patients with biliary atresia identify potential therapeutic agents. Gastroenterology. 2019;157:1138–152.e14.

18. Naoumov NV, Brees D, Loeffler J, Chng E, Ren Y, Lopez P, et al. Digital pathology with artificial intelligence analyses provides greater insights into treatment-induced fibrosis regression in NASH. J Hepatol. 2022;77:1399–409.

19. vande Casteele N, Leighton JA, Pasha SF, Cusimano F, Mookhoek A, Hagen CE, et al. Utilizing deep learning to analyze whole slide images of colonic biopsies for associations between eosinophil density and clinicopathologic features in active ulcerative colitis. Inflamm Bowel Dis. 2022;28:539–46.

20. Pai RK, Banerjee I, Shivji S, Jain S, Hartman D, Buchanan DD, et al. Quantitative pathologic analysis of digitized images of colorectal carcinoma improves prediction of recurrence-free survival. Gastroenterology. 2022;163:1531–546.e8.

21. Sjöblom N, Boyd S, Manninen A, Knuuttila A, Blom S, Färkkilä M, et al. Chronic cholestasis detection by a novel tool: Automated analysis of cytokeratin 7-stained liver specimens. Diagn Pathol. 2021;16:1–12.

22. Sjöblom N, Boyd S, Manninen A, Blom S, Knuuttila A, Färkkilä M, et al. Automated image analysis of keratin 7 staining can predict disease outcome in primary sclerosing cholangitis. Hepatol Res. 2023;53:322–33.

23. Godbole N, Nyholm I, Hukkinen M, Davidson JR, Tyraskis A, Eloranta K, et al. Prognostic and pathophysiologic significance of IL-8 (CXCL8) in biliary atresia. J Clin Med. 2021;10:2705.

24. Kerola A, Lampela H, Lohi J, Heikkilä P, Mutanen A, Hagström J, et al. Increased MMP-7 expression in biliary epithelium and serum underpins native liver fibrosis after successful portoenterostomy in biliary atresia. J Pathol Clin Res. 2016;2:187–98.

25. Nyholm I, Hukkinen M, Pihlajoki M, Davidson JR, Tyraskis A, Lohi J, et al. Serum FGF19 predicts outcomes of Kasai portoenterostomy in biliary atresia. Hepatology. 2023;77:1263–73.

26. Pozniak KN, Pearen MA, Pereira TN, Kramer CSM, Kalita-De Croft P, Nawaratna SK, et al. Taurocholate induces biliary differentiation of liver progenitor cells causing hepatic stellate cell chemotaxis in the ductular reaction: Role in pediatric cystic fibrosis liver disease. Am J Pathol. 2017;187:2744–57.

27. Sato K, Meng F, Giang T, Glaser S, Alpini G. Mechanisms of cholangiocyte responses to injury. Biochim Biophys Acta Mol Basis Dis. 2018;1864:1262–9.

28. El-Araby HA, Saber MA, Radwan NM, Taie DM, Adawy NM, Sira AM. SOX9 in biliary atresia: New insight for fibrosis progression. Hepatob Pancreat Dis Int. 2021;20:154–62.

29. Lampela H, Kosola S, Heikkilä P, Lohi J, Jalanko H, Pakarinen MP. Native liver histology after successful portoenterostomy in biliary atresia. J Clin Gastroenterol. 2013;48:721–8.

30. Clouston AD, Powell EE, Walsh MJ, Richardson MM, Demetris AJ, Jonsson JR. Fibrosis correlates with a ductular reaction in hepatitis C: Roles of impaired replication, progenitor cells and steatosis. Hepatology. 2005;41:809–18.

31. Wood MJ, Gadd VL, Powell LW, Ramm GA, Clouston AD. Ductular reaction in hereditary hemochromatosis: The link between hepatocyte senescence and fibrosis progression. Hepatology. 2014;59:848–57.

32. Overi D, Carpino G, Cristoferi L, Onori P, Kennedy L, Francis H, et al. Role of ductular reaction and ductular-canalicular junctions in identifying severe primary biliary cholangitis. JHEP Rep. 2022; 4:100556.

33. Caponcelli E, Knisely AS, Davenport M. Cystic biliary atresia: An etiologic and prognostic subgroup. J Pediatr Surg. 2008;43:1619–24.

34. Wendum D, Layese R, Ganne-Carrié N, Bourcier V, Merabtene F, Cagnot C, et al. Influence of progenitor-derived regeneration markers on hepatitis C virus–related cirrhosis outcome (ANRS CO12 CirVir Cohort). Hepatology. 2018;68:1534–48.

35. Machado MV, Michelotti GA, Pereira TA, Xie G, Premont R, Cortez-Pinto H, et al. Accumulation of duct cells with activated YAP parallels fibrosis progression in non-alcoholic fatty liver disease. J Hepatol. 2015;63:962–70.

36. Lanthier N, Rubbia-Brandt L, Lin-Marq N, Clément S, Frossard JL, Goossens N, et al. Hepatic cell proliferation plays a pivotal role in the prognosis of alcoholic hepatitis. J Hepatol. 2015;63:609–21.

37. Sancho-Bru P, Altamirano J, Rodrigo-Torres D, Coll M, Millán C, José Lozano J, et al. Liver progenitor cell markers correlate with liver damage and predict short-term mortality in patients with alcoholic hepatitis. Hepatology. 2012;55:1931–41.

38. Zagory JA, Dietz W, Park A, Fenlon M, Xu J, Utley S, et al. Notch signaling promotes ductular reactions in biliary atresia. J Surg Res. 2017;215:250–6.

39. Zagory JA, Fenlon M, Dietz W, Zhao M, Nguyen MV, Trinh P, et al. Prominin-1 promotes biliary fibrosis associated with biliary atresia. Hepatology. 2019;69:2586–97.

40. Mavila N, James D, Shivakumar P, Nguyen MV, Utley S, Mak K, et al. Expansion of prominin-1-expressing cells in association with fibrosis of biliary atresia. Hepatology. 2014;60:941–53.

41. Lin Y, Zhang F, Zhang L, Chen L, Zheng S. Characteristics of SOX9-positive progenitor-like cells during cholestatic liver regeneration in biliary atresia. Stem Cell Res Ther. 2022;13:1–11.

42. Suda H, Yoshii D, Yamamura K, Yokouchi Y, Inomata Y. New insight into reactive ductular cells of biliary atresia provided by pathological assessment of SOX9. Pediatr Surg Int. 2014;30:481–92.

43. Yoshii D, Shimata K, Yokouchi Y, Komohara Y, Suda H, Honda M, et al. SOX9 contributes to the progression of ductular reaction for the protection from chronic liver injury. Hum Cell. 2022;35:721–34.

44. Mao Y, Tang S, Yang L, Li K. Inhibition of the notch signaling pathway reduces the differentiation of hepatic progenitor cells into cholangiocytes in biliary atresia. Cell Physiol Biochem. 2018;49:1115–23.

45. Harpavat S, Hawthorne K, Setchell KDR, Narvaez Rivas M, Henn L, Beil CA, et al. Serum bile acids as a new prognostic biomarker in biliary atresia following kasai portoenterostomy. Hepatology. 2022;77:862–73.

46. Davenport M, Ong E, Sharif K, Alizai N, McClean P, Hadzic N, et al. Biliary atresia in England and Wales: Results of centralization and new benchmark. J Pediatr Surg. 2011;46:1689–94.

47. Johansson H, Svensson JF, Almström M, Van Hul N, Rudling M, Angelin B, et al. Regulation of bile acid metabolism in biliary atresia: Reduction of FGF19 by Kasai portoenterostomy and possible relation to early outcome. J Intern Med. 2020;287:534–45.